Power Control for Multigroup Multicast Cell-Free Massive MIMO Downlink

Invited Paper

Muhammad Farooq*, Markku Juntti† and Le-Nam Tran*
*School of Electrical and Electronic Engineering, University College Dublin, Ireland
Email: muhammad.farooq@ucdconnect.ie, nam.tran@ucd.ie
†Centre for Wireless Communications, University of Oulu, P.O.Box 4500, FI-90014 University of Oulu, Finland
Email: markku.juntti@oulu.fi

***Abstract*—We consider a multigroup multicast cell-free multiple-input multiple-output (MIMO) downlink system with short-term power constraints. In particular, the *normalized conjugate beamforming* scheme is adopted at each access point (AP) to keep the downlink power strictly under the power budget regardless of small scale fading. In the considered scenario, APs multicast signals to multiple groups of users whereby users in the same group receive the same message. Under this setup, we are interested in maximizing the minimum achievable rate of all groups, commonly known as the max-min fairness problem, which has not been studied before in this context. To solve the considered problem, we first present a bisection method which in fact has been widely used in previous studies for cell-free massive MIMO, and then propose an accelerated projected gradient (APG) method. We show that the proposed APG method outperforms the bisection method requiring lesser run time while still achieving the same objective value. Moreover, the considered power control scheme provides significantly improved performance and more fairness among the users compared to the equal power allocation scheme.**

***Index Terms*—Cell-free massive MIMO, multigroup multicast, max-min fairness, accelerated projected gradient**

I. Introduction

Cell-free massive multiple-input multiple-output (MIMO), where multiple users are simultaneously served by a larger number of access points (APs) in the same time spectrum resource, was first introduced in [1] and is being considered a promising technique for beyond 5G networks. In principle, cell-free massive MIMO incorporates the inherent advantages of both network MIMO and colocated massive MIMO [2], and therefore can achieve high coverage area, spectral efficiency (SE) and energy efficiency [3]. In particular, cell-free massive MIMO has the capability to provide users with nearly uniform service. Despite several benefits, scalability remains a challenge in cell-free massive MIMO since (i) the increasing number of high-capacity backhaul links are required to connect APs to the central processing unit (CPU), and (ii) large-scale resource allocation problems need to be solved at the CPU to deliver the best performance. The latter issue makes the fundamental performance of cell-free massive MIMO limited to only the small-scale systems [4].

In many practical situations, a group of users may be interested in the same information like headline news, weather update, live streaming, financial data, etc., which has motivated the study of multigroup multicast systems in massive MIMO [5], [6]. For cell-free massive MIMO, the first noticeable work in multigroup multicasting was carried out in [5], where a closed-from expression of the achievable rate for single-antenna APs and single-antenna users was derived. Moreover, the *normalized conjugate beamforming* scheme [7] was used in [5], which is devised on the basis of short-term power constraint (STPC). Note that the goal of the STPC policy is to ensure that the transmit power is always under the maximum budget regardless of instant channel gain and thus is of more practical importance [8]. This is in opposite to beamformers derived from a long-term power constraint (LTPC) policy which has been adopted in many previous studies [1], [3]. It was shown in [7] that normalized conjugate beamforming outmatches the common conjugate beamforming when the number of APs is moderate as it hardens the effective channel gains at users.

Power control for multigroup multicast cell-free massive MIMO systems has not been studied. Doan *et al.* in [5] derived the achievable rate based on the assumption that the downlink power is equally allocated to all groups, which is often termed as *equal power allocation* (EPA). In [6], Sadeghi *et al.* designed the precoders to maximize the minimum SE which is commonly known as the *max-min fairness* problem. To the best of our knowledge, no prior literature has discussed the power control for max-min fairness in multigroup multicasting cell-free massive MIMO which is our problem of interest in this paper.

In this paper, we consider a multigroup multicast cell-free MIMO downlink system using time division duplexing (TDD). Users in a group send *the same pilot sequence* to APs in the uplink for channel estimation purpose. Based on the channel estimates, APs will form different beams to different groups. In this considered system model, we derive an achievable rate in closed form and formulate the power control problem for max-min fairness based on STPC policy. To solve this problem, we first present a bisection method which is popular in the context of power control for cell-free massive MIMO [1], [3]. However, such a method is only suitable for cell-free massive MIMO of moderate sizes. To overcome this issue, we then propose a low-complexity algorithm based on the accelerated projected gradient (APG) framework [9], [10]. Simulation results demonstrate that the proposed power control algorithm can offer significant performance improvements over the EPA scheme in the considered scenarios.

*Notation*s: Standard notations are used in this paper. Bold lower and upper case letters represent vectors and matrices. $\mathcal{CN}(\mathbf{0},\mathbf{R})$ denotes the multivariate circularly symmetric complex Gaussian random distribution with zero mean and covariance matrix $\mathbf{R}$. $\mathbb{R}^{x\times y}$ represents the space of real matrices with the dimensions $x\times y$. $\mathbf{X}^*$, $\mathbf{X}^{\mathrm{T}}$ and $\mathbf{X}^{\dagger}$ stand for the conjugate, transpose and conjugate transpose (Hermitian) of $\mathbf{X}$, respectively. The "+" sign in the subscript of a space implies that all elements of that space are positive. $\mathbb{E}\{X\}$ denotes the expectation or mean of random variable X. x_i is the i-th entry of vector $\mathbf{x}$; $[\mathbf{X}]_{i,j}$ is the entry at the i-th row and j-th column of $\mathbf{X}$. $\|\cdot\|$ represents the Euclidean norm; $|\cdot|$ is the absolute value of the argument. The operator diag converts a vector intro a diagonal matrix. $\mathbf{I}_N$ is the $N\times N$ identity matrix. $\ln(\cdot)$ denotes the natural logarithm.

II. System Model and Problem Formulation

A. System Model

Consider a cell-free massive MIMO scenario where M single-antenna APs are connected to a CPU via a perfect back-haul link. The APs coherently transmit N independent messages to N groups of users in a TDD mode. Note that all users in the same group receive the same message. The number of single-antenna users in the n-th group is denoted by K_n. Throughout the paper, we note that the notation n_k refers to the k-th user in the n-th group. In this regard, the channel coefficient between the m-th AP and the k-th user in the n-th group is modeled as

$$h_{mn_k}=\zeta_{mn_k}^{1/2}g_{mn_k}, \tag{1}$$

where ζ_{mn_k} and g_{mn_k} represent the large-scale and small-scale fading coefficients, respectively. We further assume that $g_{mn_k}, m=1,2,\ldots,M, n=1,2,\ldots,N, k=1,2,\ldots,K_n$, are independent identically distributed (i.i.d) $\mathcal{CN}(0,1)$ random variables. In this paper, we also assume that no downlink pilots will be sent from APs to users. Thus, the transmission in one coherence time, denoted by τ_c symbols, only includes the uplink training phase and data multicasting phase which are described in the following subsections.

1) Uplink Training: Since the TDD mode is adopted and the transmission takes place within one coherence interval, the channel can be considered reciprocal, i.e., the channel gains on the uplink and on the downlink are deem to be identical. Consequently, the APs can estimate the downlink channel based on the pilot sequences sent by all users on the uplink. Let $\sqrt{\tau_p}\boldsymbol{\psi}_n\in\mathbb{C}^{T_p\times 1}$, where $\boldsymbol{\psi}_n$ be the *common pilot sequence* transmitted from all users in the n-th group, where τ_p is the length of the pilot sequences in symbols. These pilot sequences are assumed to be independent and orthonormal (i.e., $\|\boldsymbol{\psi}_n\|^2=1,\forall n$ and $\boldsymbol{\psi}_n^{\dagger}\boldsymbol{\psi}_{n'}=0, n'\neq n$) among N groups and thus, the effect of pilot contamination is ignored. The received signal at the m-th AP is given by

$$\mathbf{y}_m=\sqrt{\rho_p\tau_p}\sum_{n=1}^{N}\sum_{k=1}^{K_n}h_{mn_k}\boldsymbol{\psi}_n+\mathbf{w}_m, \tag{2}$$

where ρ_p is the power of each pilot symbol, and $\mathbf{w}_m\sim\mathcal{CN}(\mathbf{0},\sigma_n^2\mathbf{I}_{T_p})$ is the noise and σ_n^2 is the variance of the noise sample. The m-th AP needs to estimate the channel h_{mn_k}, based on the received pilot signal $\mathbf{y}_m$. In fact, this process is described in [5] and is re-derived here with further details to be self-contained. Specifically, the m-th AP projects $\mathbf{y}_m$ onto $\boldsymbol{\psi}_n$, producing

$$\tilde{y}_{mn}=\boldsymbol{\psi}_n^{\dagger}\mathbf{y}_m=\sqrt{\rho_p\tau_p}\sum_{k=1}^{K_n}h_{mn_k}+\tilde{w}_{mn}, \tag{3}$$

where $\tilde{w}_{mn}\triangleq\boldsymbol{\psi}_n^{\dagger}\mathbf{w}_m\sim\mathcal{CN}(0,\sigma_n^2)$. The minimum mean-square error (MMSE) of the channel estimate is calculated as

$$\hat{h}_{mn_k}=\frac{\mathbb{E}\{h_{mn_k}\tilde{y}_{mn}\}}{\mathbb{E}\{\tilde{y}_{mn}^2\}}\tilde{y}_{mn}=\frac{\sqrt{\rho_p\tau_p}\zeta_{mn_k}}{\rho_p\tau_p\sum_{l=1}^{K_n}\zeta_{mn_l}+\sigma_n^2}\tilde{y}_{mn}. \tag{4}$$

Note that the expectations in the above equation are carried out with respect to small-scale fading. Since the elements of $\hat{h}_{mn_k}$ are independent and identical Gaussian distribution, we can write it as $\hat{h}_{mn_k}=\gamma_{mn_k}^{1/2}z_{mn}$, where $\gamma_{mk}=\frac{\rho_p\tau_p\zeta_{mn_k}^2}{\sigma_n^2+\rho_p\tau_p\sum_{l=1}^{K_n}\zeta_{mn_l}}$ and $z_{mn}=\frac{\tilde{y}_{mn}}{\sqrt{\rho_p\tau_p\sum_{l=1}^{K_n}\zeta_{mn_l}+\sigma_n^2}}\sim\mathcal{CN}(0,1)$.

2) Downlink Multicasting: For the downlink multicasting phase, the APs use the channel estimates obtained in (4) to form separate radio beams to the N groups. Similar to [5], we adopt *normalized conjugate beamforming* under the STPC. More specifically, we denote the symbol to be sent to the n-th group by s_n such that $\mathbb{E}\{|s_n|^2\}=1$. Then the transmitted symbol from the m-th AP is given by

$$x_m=\sqrt{\rho_d}\sum\nolimits_{n=1}^{N}\sqrt{\eta_{mn}}\frac{z_{mn}^*}{|z_{mn}|}s_n, \tag{5}$$

where η_{mn} is the power control coefficient between the m-th AP and the n-th group and ρ_d is the maximum power at each AP. Note that the factor $\frac{z_{mn}^*}{|z_{mn}|}$ in the above is known as normalized conjugate beamforming which incorporates STPC. Explicitly, the total power constraint at each AP is

$$\mathbb{E}\{|x_m|^2\}=\rho_d\sum\nolimits_{n=1}^{N}\eta_{mn}, \tag{6}$$

which is *independent* of the small-scale fading coefficient. We remark that power control is not considered in [5]. Finally, the received signal at the k-th user in the n-th group is written as

$$\begin{aligned}r_{n_k}&=\sum_{m=1}^{M}h_{mn_k}x_m+w_{n_k}\\&=\sqrt{\rho_d}a_{n_k}s_n+\sqrt{\rho_d}\sum_{n'\neq n}^{N}a_{n'_k}s_{n'}+w_{n_k},\end{aligned} \tag{7}$$

where $a_{n_k} = \sum_{m=1}^{M} h_{mn_k}\sqrt{\eta_{mn}}\frac{z_{mn}^*}{|z_{mn}|}$, $a_{n'_k} = \sum_{m=1}^{M} h_{mn_k}\sqrt{\eta_{mn'}}\frac{z_{mn'}^*}{|z_{mn'}|}$, and $w_{n_k} \sim \mathcal{CN}(0,\sigma_n^2)$ is the additive thermal noise.

3) Signal Detection based on Channel Statistics and Spectral Efficiency: The k-th user in group n will rely on the mean of the effective channel gain to detect s_n. To see this we rewrite (7) as

$$r_{n_k} = \sqrt{\rho_d}\ \mathbb{E}\{a_{n_k}\}s_n + \sqrt{\rho_d}\ \big(a_{n_k} - \mathbb{E}\{a_{n_k}\}\big)s_n + \sqrt{\rho_d}\sum_{n'\neq n}^{N} a_{n'_k}s_{n'} + w_{n_k}. \quad (8)$$

As in [5], we use the worst-case Gaussian noise argument given in [11, section 2.3.4] to obtain the achievable rate (nat/s/Hz) which is expressed as

$$\mathcal{R}_{n_k} = \ln\bigg(1 + \frac{\rho_d|\mathbb{E}\{a_{n_k}\}|^2}{\rho_d\,\mathbb{V}\mathrm{ar}\{a_{n_k}\} + \rho_d\sum_{n'\neq n}^{N}\big|\mathbb{E}\{a_{n'_k}\}\big|^2 + \sigma_n^2}\bigg). \quad (9)$$

Proposition 1. *For a multigroup multicast scenario using the normalized conjugate beamforming, the achievable rate for user k in group n in* (9) *is reduced to*

$$\mathcal{R}_{n_k} = \ln\bigg(1 + \frac{\frac{\pi\rho_d}{4}\big(\sum_{m=1}^{M}\sqrt{\eta_{mn}\gamma_{mn_k}}\big)^2}{\rho_d\sum_{m=1}^{M}\eta_{mn}(N\zeta_{mn_k} - \frac{\pi}{4}\gamma_{mn_k}) + \sigma_n^2}\bigg). \quad (10)$$

Proof: The proof follows the same arguments as those in [5, Appendix A], and, thus, is omitted here due to the space limitation. We remark that when the power control coefficients are $\eta_{mn} = \frac{1}{N}$, i.e., EPA, the achievable rate in (10) becomes

$$\mathcal{R}_{n_k} = \ln\bigg(1 + \frac{\frac{\pi\rho_d}{4N}\big(\sum_{m=1}^{M}\sqrt{\gamma_{mn_k}}\big)^2}{\rho_d\sum_{m=1}^{M}\big(\zeta_{mn_k} - \frac{\pi}{4N}\gamma_{mn_k}\big) + \sigma_n^2}\bigg), \quad (11)$$

which is in fact [5, Eq. (14)]. ■

B. Max-min Fairness Power Control

To ensure the fairness among all the users, we consider the problem of max-min fairness. Inspired from [10], [12], for the purpose of developing an efficient numerical method, we define $\mu_{mn} = \sqrt{\eta_{mn}}, \forall m, \forall n$. As a result, the achievable rate in (10) is equivalently rewritten as

$$\mathcal{R}_{n_k}(\boldsymbol{\mu}) = \frac{\frac{\pi\rho_d}{4}\big(\sum_{m=1}^{M}\mu_{mn}\sqrt{\gamma_{mn_k}}\big)^2}{\rho_d\sum_{m=1}^{M}\mu_{mn}^2\big(N\zeta_{mn_k} - \frac{\pi}{4}\gamma_{mn_k}\big) + \sigma_n^2}, \quad (12)$$

where $\boldsymbol{\mu} \triangleq [\boldsymbol{\mu}_1;\boldsymbol{\mu}_2;\ldots;\boldsymbol{\mu}_N] \in \mathbb{R}^{MN}$, and $\boldsymbol{\mu}_n \triangleq [\mu_{1n};\mu_{2n};\ldots;\mu_{Mn}] \in \mathbb{R}^M, \forall n$. To ensure that the total transmit power at each AP does not exceed ρ_d, we impose the constrain $\sum_{n=1}^{N}\eta_{mn} \leq 1$, which is equivalent to $\sum_{n=1}^{N}\mu_{mn}^2 \leq 1, \forall m$. The considered power control problem can be mathematically stated as

$$\begin{aligned} \underset{\boldsymbol{\mu}}{\text{maximize}} \quad & f(\boldsymbol{\mu}) = \min_{\forall n_k} \mathcal{R}_{n_k}(\boldsymbol{\mu}) \\ \text{subject to} \quad & \textstyle\sum_{n=1}^{N}\mu_{mn}^2 \leq 1, \forall m \\ & \mu_{mn} \geq 0, \forall m, \forall n. \end{aligned} \quad (\mathcal{P})$$

III. Proposed Solution

In this section, we propose a low-complexity method for solving ($\mathcal{P}$). Before doing this, we note that $\mathcal{R}_{n_k}(\boldsymbol{\mu})$ is in fact quasi-concave and thus, a bisection method can be applied to solve ($\mathcal{P}$). To see that, we first rewrite ($\mathcal{P}$) as

$$\begin{aligned} \underset{\boldsymbol{\mu}}{\text{maximize}} \quad & t \\ \text{subject to} \quad & \textstyle\sum_{n=1}^{N}\mu_{mn}^2 \leq 1, \forall m \\ & \mathcal{R}_{n_k}(\boldsymbol{\mu}) \geq t, \forall n_k \\ & \mu_{mn} \geq 0, \forall m, \forall n. \end{aligned} \quad (13)$$

It is easy to see that the constraint $\mathcal{R}_{n_k}(\boldsymbol{\mu}) \geq t$ is equivalent to

$$\sqrt{\frac{\pi\rho_d}{4}}\big(\textstyle\sum_{m=1}^{M}\mu_{mn}\sqrt{\gamma_{mn_k}}\big) \geq \sqrt{e^t - 1}\sqrt{\rho_d\textstyle\sum_{m=1}^{M}\mu_{mn}^2\big(N\zeta_{mn_k} - \frac{\pi}{4}\gamma_{mn_k}\big) + \sigma_n^2}. \quad (14)$$

For a given t, the above constraint is indeed a second order cone constraint. Hence, a bisection search over t can be used to find the optimal solution. However, the problem with such a method is that it has high computational complexity which makes it less appealing to large-scale problems. In what follows, we present solutions to ($\mathcal{P}$) using an APG method introduced in [9]. For efficiently description of the proposed method, we first reformulate the problem in the form of a single vector of power control coefficients as described next.

A. Smoothing Technique

Let us denote $\bar{\boldsymbol{\mu}}_m = [\mu_{m1};\mu_{m2};\ldots;\mu_{mN}] \in \mathbb{R}^N$ which include all power control coefficients associated with the m-th AP. The the feasible set in ($\mathcal{P}$) can be expressed as

$$\mathcal{S} = \{\boldsymbol{\mu}|\boldsymbol{\mu} \geq 0; \|\bar{\boldsymbol{\mu}}_m\|^2 \leq 1, \forall m\}. \quad (15)$$

Also, to simply the mathematical presentation, we first rewrite $\mathcal{R}_{n_k}(\boldsymbol{\mu})$ in a more compact form of $\boldsymbol{\mu}$ as

$$\mathcal{R}_{n_k}(\boldsymbol{\mu}) = \ln\bigg(1 + \frac{\frac{\pi\rho_d}{4}(\boldsymbol{\gamma}_{n_k}^{\mathrm{T}}\boldsymbol{\mu}_n)^2}{\rho_d\|\mathbf{A}_{n_k}\boldsymbol{\mu}_n\|^2 + 1}\bigg), \quad (16)$$

where $\mathbf{A}_{n_k}$ is the diagonal defined as

$$\mathbf{A}_{n_k} = \mathrm{diag}\bigg(\Big[\sqrt{N\zeta_{1n_k} - \frac{\pi}{4}\gamma_{1n_k}}; \sqrt{N\zeta_{2n_k} - \frac{\pi}{4}\gamma_{2n_k}}; \ldots; \sqrt{N\zeta_{Mn_k} - \frac{\pi}{4}\gamma_{Mn_k}}\Big]\bigg). \quad (17)$$

It is important to note that the objective $f(\boldsymbol{\mu})$ ($\mathcal{P}$) is *nonsmooth,* which is a preliminary requirement for an application of a gradient-based method. To overcome this issue, we use the smoothing technique introduced in [13]. Specifically, for a given *smoothness* parameter $\sigma > 0$, $f(\boldsymbol{\mu})$ is approximated by the following log-sum-exp function [13]

$$f_\sigma(\boldsymbol{\mu}) = -\frac{1}{\sigma}\ln\Big(\frac{1}{NK_n}\textstyle\sum_{n=1}^{N}\sum_{k=1}^{K_n}\exp\big(-\sigma\mathcal{R}_{n_k}(\boldsymbol{\mu})\big)\Big). \quad (18)$$

In [13], Nesterov proved that $f_\sigma(\boldsymbol{\mu})$ is a differentiable approximation of $f(\boldsymbol{\mu})$ with a numerical accuracy of $\frac{\ln(NK_n)}{\tau}$, i.e., $f(\boldsymbol{\mu}) \leq f_\sigma(\boldsymbol{\mu}) \leq f(\boldsymbol{\mu}) + \frac{\ln(NK_n)}{\sigma}$. Hence, with a sufficiently large value of σ, $f(\boldsymbol{\mu})$ can be replaced with $f_\sigma(\boldsymbol{\mu})$ for the optimization purpose. In this way, $(\mathcal{P})$ is approximated by

$$\begin{aligned} \underset{\boldsymbol{\mu}}{\text{maximize}} \quad & f_\sigma(\boldsymbol{\mu}) \\ \text{subject to} \quad & \boldsymbol{\mu} \in \mathcal{S}. \end{aligned} \tag{$\hat{\mathcal{P}}$}$$

In addition to the smoothness of $f_\sigma(\boldsymbol{\mu})$, the projection onto $\mathcal{S}$ can be done in closed form as shall be seen shortly. This motivates us to apply the APG method in [9] to solve $(\hat{\mathcal{P}})$.

B. Proposed Accelerated Projected Gradient Method

The proposed algorithm for solving $(\hat{\mathcal{P}})$ is outlined in Algorithm 1. From (18), the gradient of $f_\sigma(\boldsymbol{\mu})$ is found as

Algorithm 1: Proposed APG Algorithm

Input: $\mathbf{z}^1 = \boldsymbol{\mu}^1 = \boldsymbol{\mu}^0 > 0$, $\sigma >> 1$, $\delta > 0$, $\alpha_y^0 > 0$, $\alpha_\mu^0 > 0$, $0 < \kappa < 1$

for $n = 1, 2, \cdots$ **do**

Find extrapolated point $\mathbf{y}^n$, where $\mathbf{y}^n = \boldsymbol{\mu}^n + \frac{t_{n-1}}{t_n}(\mathbf{z}^n - \boldsymbol{\mu}^n) + \frac{t_{n-1}-1}{t_n}(\boldsymbol{\mu}^n - \boldsymbol{\mu}^{n-1})$.

Find the smallest nonnegative integer l_y and $\mathbf{z}^{n+1}$ such that $f_\sigma(\mathbf{z}^{n+1}) \geq f_\sigma(\mathbf{y}^n) + \delta\left\|\mathbf{z}^{n+1} - \mathbf{y}^n\right\|^2$, where $\mathbf{z}^{n+1} = P_{\mathcal{S}}(\mathbf{y}^n + \kappa^{l_y}\alpha_y^{n-1}\nabla f_\sigma(\mathbf{y}^n))$.

Find the smallest nonnegative integer l_μ and $\mathbf{v}^{n+1}$ such that $f_\sigma(\mathbf{v}^{n+1}) \geq f_\sigma(\boldsymbol{\mu}^n) + \delta\left\|\mathbf{v}^{n+1} - \boldsymbol{\mu}^n\right\|^2$, where $\mathbf{v}^{n+1} = P_{\mathcal{S}}(\boldsymbol{\mu}^n + \kappa^{l_\mu}\alpha_\mu^{n-1}\nabla f_\sigma(\boldsymbol{\mu}^n))$.

Set $\alpha_y^n = \kappa^{l_y}\alpha_y^{n-1}$, $\alpha_\mu^n = \kappa^{l_\mu}\alpha_\mu^{n-1}$, and extrapolation parameter $t_{n+1} \triangleq 0.5 + \sqrt{t_n^2 + 0.25}$.

if $f_\sigma(\mathbf{z}^{n+1}) > f_\sigma(\mathbf{v}^{n+1})$ **then**

$\boldsymbol{\mu}^{n+1} = \mathbf{z}^{n+1}$

else

$\boldsymbol{\mu}^{n+1} = \mathbf{v}^{n+1}$

end

end

$$\frac{\partial}{\partial\boldsymbol{\mu}} f_\sigma(\boldsymbol{\mu}) = \frac{\sum_{n=1}^{N}\sum_{k=1}^{K_n}\Big(\exp\big(-\sigma\mathcal{R}_{n_k}(\boldsymbol{\mu})\big)\nabla_{\boldsymbol{\mu}}\mathcal{R}_{n_k}(\boldsymbol{\mu})\Big)}{\sum_{n=1}^{N}\sum_{k=1}^{K_n}\exp\big(-\sigma\mathcal{R}_{n_k}(\boldsymbol{\mu})\big)}. \tag{19}$$

It is easy to see that the gradient of $\mathcal{R}_{n_k}(\boldsymbol{\mu})$ is

$$\nabla_{\boldsymbol{\mu}}\mathcal{R}_{n_k}(\boldsymbol{\mu}) = \frac{\nabla_{\boldsymbol{\mu}}\big(b_{n_k}(\boldsymbol{\mu}_n) + c_{n_k}(\boldsymbol{\mu}_n)\big)}{b_{n_k}(\boldsymbol{\mu}_n) + c_{n_k}(\boldsymbol{\mu}_n)} - \frac{\nabla_{\boldsymbol{\mu}} c_{n_k}(\boldsymbol{\mu}_n)}{c_{n_k}(\boldsymbol{\mu}_n)}, \tag{20}$$

where $b_{n_k}(\boldsymbol{\mu}_n) \triangleq \frac{\pi\rho_d}{4}(\boldsymbol{\gamma}_{n_k}^{\mathrm{T}}\boldsymbol{\mu}_n)^2$ and $c_{n_k}(\boldsymbol{\mu}_n) \triangleq \rho_d\|\mathbf{A}_{n_k}\boldsymbol{\mu}_n\|^2 + 1$. By recalling the identity $\nabla_{\mathbf{x}}\|\mathbf{A}\mathbf{x}\|^2 = 2\mathbf{A}^{\mathrm{T}}\mathbf{A}\mathbf{x}$ for any symmetric matrix $\mathbf{A}$, the gradients $\nabla_{\boldsymbol{\mu}} b_{n_k}(\boldsymbol{\mu}_n)$ and $\nabla_{\boldsymbol{\mu}} c_{n_k}(\boldsymbol{\mu}_n)$ in the above equation are calculated as

$$\nabla_{\boldsymbol{\mu}} b_{n_k}(\boldsymbol{\mu}_n) = \frac{\pi\rho_d}{2}\boldsymbol{\gamma}_{n_k}\boldsymbol{\gamma}_{n_k}^{\mathrm{T}}\boldsymbol{\mu}_n, \tag{21}$$

$$\nabla_{\boldsymbol{\mu}} c_k(\boldsymbol{\mu}) = 2\rho_d\mathbf{A}_{n_k}^{\mathrm{T}}\mathbf{A}_{n_k}\boldsymbol{\mu}_n. \tag{22}$$

Further note that the projection of any vector $\mathbf{x}$ onto the $\mathcal{S}$ is defined as

$$P_{\mathcal{S}}(\mathbf{x}) = \arg\min\big\{||\mathbf{x} - \mathbf{u}|| \mid \mathbf{u} \in \mathcal{S}\big\}. \tag{23}$$

The Euclidean projection onto $\mathcal{S}$ defined in (23) can be done can be done *in parallel* and by *closed-form expressions*. In particular, the optimization problem in (23) can be decomposed into sub-problems at each AP m as

$$\bar{\boldsymbol{\mu}}_m = \arg\min\big\{||\bar{\mathbf{x}}_m - \bar{\boldsymbol{\mu}}_m|| \mid \|\bar{\boldsymbol{\mu}}_m\|^2 \leq 1, \bar{\boldsymbol{\mu}}_m \geq 0\big\}, \tag{24}$$

where $\bar{\mathbf{x}}_m = [x_{m1}; x_{m2}; \ldots; x_{mN}] \in \mathbb{R}^N$. The above problem can solved by finding the projection onto the intersection of the positive orthant and Euclidean ball [14, Theorem 7.1]. More specifically, we first project $\bar{\mathbf{x}}_m$ onto the positive orthant, i.e., $[\bar{\mathbf{x}}_m]_+$ and then onto the unit-norm ball which is simply given by

$$\bar{\boldsymbol{\mu}}_m = \begin{cases} [\bar{\mathbf{x}}_m]_+ & \|[\bar{\mathbf{x}}_m]_+\| \leq 1, \\ \frac{[\bar{\mathbf{x}}_m]_+}{\|[\bar{\mathbf{x}}_m]_+\|} & \text{otherwise.} \end{cases} \tag{25}$$

C. Complexity Analysis

Now, we describe the complexity of the proposed algorithm using the big-O notation. Note that for each general step in Algorithm 1, three factors contribute towards the computational complexity; the objective (18), the gradient (19) and the projection (25). It can be easily verified that the computation of $\mathcal{R}_{n_k}$ requires M multiplications and therefore, the complexity of finding the objective is $\mathcal{O}\big(M\sum_{n=1}^{N}K_n\big)$. Similarly the gradient $\frac{\partial}{\partial\boldsymbol{\mu}}f_\sigma(\boldsymbol{\mu})$ has the complexity of $\mathcal{O}\big(M\sum_{n=1}^{N}K_n\big)$ also. The projection operation requires the computation of l_2-norm of $\mathbb{R}^N$ vectors at all M APs and thus, has complexity of $\mathcal{O}(MN)$. In summary, the per-iteration complexity of the proposed algorithm is $\mathcal{O}\big(M\sum_{n=1}^{N}K_n\big)$.

IV. Numerical Results

In this section, we evaluate the performance of the proposed method in different multigroup multicasting cell-free massive MIMO scenarios. The system bandwidth is set to $B = 20\,\text{MHz}$ and the carrier frequency to $f = 1900\,\text{MHz}$. We generate the channel in (1) similar to [5], where $\sigma_{\text{sh}} = 9$ dB be the standard deviation of the log-normal shadowing. Also, the noise power is calculated as $N_0 = k \times T \times B \times NF$, where $NF = 9\,\text{dB}$ is the noise figure, $T = 290\,\text{K}$ is the temperature, and $k = 1.38 \times 10^{-23}\text{J/K}$ is the Boltzmann's constant. Further, we choose $\rho_d = \rho_p = 0.2\,\text{W}$, $\tau_p = 20$, $\tau_c = 200$ and $K_n = K$ (i.e., same number of users for each group) in all the experiments. APs and users are distributed uniformly over the area of $D = 1\,\text{km}^2$. The parameters involved in Algorithm 1 are set to $\sigma = 100$, $\delta = 10^{-5}$ and $\kappa = 0.45$.

First, we plot in Fig. 1 the achieved minimum rate of all users using Algorithm 1 for two different scenarios. Note that one set of channel realizations is randomly generated for each scenario. In particular, we compare the convergence of the proposed APG method with the the bisection method. To solve the resulting feasibility problem in each iteration of the bisection method, we use the modeling tool CVX [15]. It can be observed from the Fig. 1 that the proposed method reaches the same objective value as the bisection method. The advantage of Algorithm 1 is that it takes much less run time than the bisection method to return a solution as recorded in Table I. Particularly, the bisection method cannot handle

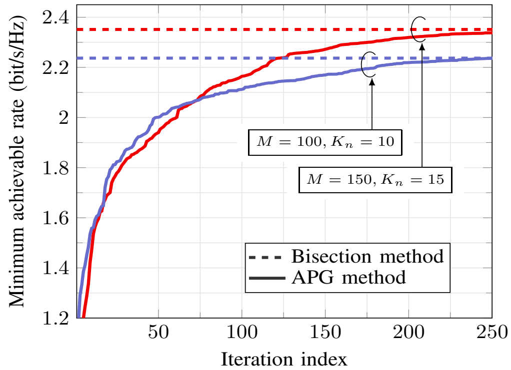

Fig. 1. Comparison of convergence of Algorithm 1 with the bisection method for two scenarios; $M = 100, K_n = 10$ and $M = 150, K_n = 15$. Here, we consider four groups with $K_n = K$ users in each group.

large-scale scenarios due to the large required memory and extremely long run time.

TABLE I
COMPARISON OF RUN-TIME (IN SECONDS) FOR $N = 2$ AND $K_n = 15$.

APs	Bisection Method	Proposed APG Method
100	54.77	**6.43**
150	68.50	**13.58**
200	103.75	**26.69**

Next, we demonstrate the benefits of power control optimization for multigroup multicast cell-free massive MIMO systems. To this end, we plot in Fig. 2 the achieved cumulative distribution function (CDF) of per-user rate using the proposed power control algorithm and compare it with the EPA scheme in [5]. The results shown in Fig. 2 are interesting in many

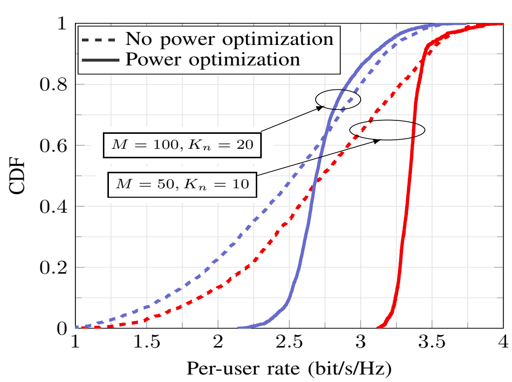

Fig. 2. CDF for the considered power control scheme compared with the EPA scheme. In the experiment, we take $N = 2$ and simulate two scenarios; $M = 50, K = 10$ and $M = 100, K = 20$.

ways. First, the considered power control scheme outperform the EPA method in terms of performance for both considered scenarios. Another observation is that Algorithm 1 is better in terms of fairness among the users. Note that for the fixed area, the per-user rate decreases as the problem size increases. This is due to the fact that with an increase in the number of users, the inter-user interference among the users of the different groups increases which in turn causes a significant decrease in the achievable rate.

V. CONCLUSION

We have considered the max-min fairness problem in the downlink channel of multigroup multicasting cell-free massive MIMO. We have formulated the power control problem using normalized conjugated beamforming scheme which incorporates the STPC to strictly constrain the downlink power to stay under maximum allowable power at each AP. To solve the problem, we have proposed a low-complexity algorithm based on the APG iterations. Our simulation results have shown that the proposed algorithm achieves the same objective as the well-known bisection algorithm but in much lesser run time. More specially, the proposed APG method outperforms the EPA method both in terms of achievable rate fairness among the users.

ACKNOWLEDGMENT

This publication has emanated from research supported by a Grant from Science Foundation Ireland under Grant number 17/CDA/4786.

REFERENCES

[1] H. Q. Ngo, A. Ashikhmin, H. Yang, E. G. Larsson, and T. L. Marzetta, "Cell-free massive MIMO versus small cells," *IEEE Trans. Wireless Commun.*, vol. 16, no. 3, pp. 1834–1850, Mar. 2017.

[2] T. L. Marzetta, "Noncooperative cellular wireless with unlimited numbers of base station antennas," *IEEE Trans. Wireless Commun.*, vol. 9, no. 11, pp. 3590–3600, Nov. 2010.

[3] H. Q. Ngo, L. Tran, T. Q. Duong, M. Matthaiou, and E. G. Larsson, "On the total energy efficiency of cell-free massive MIMO," *IEEE Trans. Green Commun. Netw.*, vol. 2, no. 1, pp. 25–39, Mar. 2018.

[4] M. Bashar, K. Cumanan, A. G. Burr, H. Q. Ngo, and M. Debbah, "Cell-free massive MIMO with limited backhaul," in *IEEE ICC 2018*, 2018, pp. 1–7.

[5] T. X. Doan, H. Q. Ngo, T. Q. Duong, and K. Tourki, "On the performance of multigroup multicast cell-free massive MIMO," *IEEE Commun. Lett.*, vol. 21, no. 12, pp. 2642–2645, 2017.

[6] M. Sadeghi, E. Björnson, E. G. Larsson, C. Yuen, and T. L. Marzetta, "Max–min fair transmit precoding for multi-group multicasting in massive MIMO," *IEEE Wireless Commun. Lett.*, vol. 17, no. 2, pp. 1358–1373, 2018.

[7] G. Interdonato, H. Q. Ngo, E. G. Larsson, and P. Frenger, "On the performance of cell-free massive MIMO with short-term power constraints," in *IEEE CAMAD 2016*, 2016, pp. 225–230.

[8] M. Khoshnevisan and J. N. Laneman, "Power allocation in wireless systems subject to long-term and short-term power constraints," in *IEEE ICC 2011*, 2011, pp. 1–5.

[9] H. Li and Z. Lin, "Accelerated proximal gradient methods for nonconvex programming," in *Advances in Neural Information Processing Systems 28*, C. Cortes, N. D. Lawrence, D. D. Lee, M. Sugiyama, and R. Garnett, Eds. Curran Associates, Inc., 2015, pp. 379–387.

[10] M. Farooq, H. Q. Ngo, and L.-N. Tran, "Accelerated projected gradient method for the optimization of cell-free massive MIMO downlink," in *Proc. IEEE PIMRC 2020*, 2020, pp. 1–6.

[11] T. L. Marzetta, E. G. Larsson, H. Yang, and H. Q. Ngo, *Fundamentals of Massive MIMO*. Cambridge University Press, 2016.

[12] L. Tran and H. Q. Ngo, "First-order methods for energy-efficient power control in cell-free massive MIMO," in *Proc. IEEE ACSSC 2019*, 2019, pp. 848–852.

[13] Y. Nesterov, "Smooth minimization of non-smooth functions," *Math. Program., Ser. A*, vol. 103, pp. 127–152, 2005.

[14] H. H. Bauschke, M. N. Bui, and X. Wang, "Projecting onto the intersection of a cone and a sphere," *SIAM Journal on Optimization*, vol. 28, no. 3, pp. 2158–2188, Jan. 2018.

[15] M. Grant and S. Boyd, "CVX: Matlab software for disciplined convex programming, version 1.21," http://cvxr.com/cvx, Apr. 2011.